




Article

Physical, Structural, Barrier, and Antifungal Characterization of Chitosan–Zein Edible Films with Added Essential Oils

Monserrat Escamilla-García ¹, Georgina Calderón-Domínguez ², Jorge J. Chanona-Pérez ²,
Angélica G. Mendoza-Madrigal ³, Prospero Di Pierro ⁴, Blanca E. García-Almendárez ¹,
Aldo Amaro-Reyes ¹ and Carlos Regalado-González ^{1,*} 

¹ Department of Food Research and Postgraduate Studies, C.U., Autonomous University of Querétaro, Cerro de las Campanas S/N, Las Campanas, Santiago de Querétaro 76010, Mexico; moneg14@hotmail.com (M.E.-G.); blancag31@gmail.com (B.E.G.-A.); aldoamaro@gmail.com (A.A.-R.)

² Department of Biochemical Engineering, National Polytechnic Institute, Av. Wilfrido Massieu Esq. Cda. Miguel Stampa S/N, Gustavo A. Madero, Ciudad de México 07738, Mexico; ginacaldero@hotmail.com (G.C.-D.); jorge_chanona@hotmail.com (J.J.C.-P.)

³ Faculty of Nutrition, Research Laboratory, Autonomous University of the State of Morelos, Vista Hermosa S/N, Cuernavaca 62350, Mexico; gabriela.mendoza@uaem.mx

⁴ Department of Chemical Sciences, University of Naples “Federico II”, Complesso Universitario di Monte Sant’Angelo, Via Cinthia, 21, 80126 Napoli, Italy; prospero.dipierro@unina.it

* Correspondence: regcarlos@gmail.com; Tel.: +52-442-123-8332

Received: 13 October 2017; Accepted: 2 November 2017; Published: 8 November 2017

Abstract: Edible films (EFs) have gained great interest due to their ability to keep foods safe, maintaining their physical and organoleptic properties for a longer time. The aim of this work was to develop EFs based on a chitosan–zein mixture with three different essential oils (EOs) added: anise, orange, and cinnamon, and to characterize them to establish the relationship between their structural and physical properties. The addition of an EO into an EF significantly affected ($p < 0.05$) the a^* (redness/greenness) and b^* (yellowness/blueness) values of the film surface. The EFs presented a refractive index between 1.35 and 1.55, and thus are classified as transparent. The physical properties of EFs with an added EO were improved, and films that incorporated the anise EO showed significantly lower water vapor permeability ($1.2 \pm 0.1 \text{ g mm h}^{-1} \text{ m}^{-2} \text{ kPa}^{-1}$) and high hardness ($104.3 \pm 3.22 \text{ MPa}$). EFs with an added EO were able to inhibit the growth of *Penicillium* sp. and *Rhizopus* sp. to a larger extent than without an EO. Films’ structural changes were the result of chemical interactions among amino acid side chains from zein, glucosamine from chitosan, and cinnamaldehyde, anethole, or limonene from the EOs as detected by a Raman analysis. The incorporation of an EO in the EFs’ formulation could represent an alternative use as coatings to enhance the shelf life of food products.

Keywords: essential oils; edible films; raman spectroscopy; chitosan; zein; *Rhizopus*; *Penicillium*

1. Introduction

The growing demand for high-quality and safe foods is leading to increased synthetic packaging materials production. However, there are environmental concerns about their use despite the benefits they provide, such as preserving and ensuring food quality [1]. Edible films (EFs) may be an alternative to reduce the use of synthetic polymers, while the addition of essential oils (EO) may improve physical and antimicrobial properties [2]. EOs have been extensively studied as natural products to provide benefits in food and human health. EOs or their components can be added directly to foods or

incorporated into containers made of non-renewable materials, or biomaterials, such as polypropylene or chitosan, respectively, to be released during transport and storage [3].

Cinnamaldehyde is the major active component of the cinnamon EO (CN), and has shown a broad antimicrobial spectrum against bacteria, yeasts, and molds. Thus, CN could be used as a natural food preservative, and may be added into edible coatings to improve the shelf life and safety of food products [4]. There have been reports on the bactericidal effect of CN against *Salmonella*, *Campylobacter*, *Escherichia coli* O157:H7, and *Listeria monocytogenes*, and its antifungal activity against *Aspergillus* sp., *Penicillium* sp., and *Colletotrichum* sp. [5,6].

There is increased interest in the use of the anise EO (AS) due to its antioxidant capacity and antifungal effect against *Penicillium* sp. and *Aspergillus* sp. [7]. Anethole is the major active component of AS [8], which has been incorporated into edible coatings for dried fish and fruits preservation [9]. Limonene is the main component of the orange EO (OR), and has shown insecticidal, antibacterial, and antifungal activities. It has shown activity against *Streptococcus* sp., *Aspergillus* sp., and *Penicillium* sp. [10,11]. Limonene has many applications in both the food and cosmetic industries, but due to its lipophilic character, it exhibits poor water absorption, palatability, and oxidative deterioration [12].

The Food and Drug Administration of the U.S. lists all of the essential oils used in this work as Generally Recognized as Safe (GRAS). Water vapor permeability and the migration of atmospheric gases are dependent on many interrelated factors, including the polarity and structural features of polymers' side chains, hydrogen bonding characteristics, the degree of branching or cross-linking, and the degree of crystallinity [13]. The spatial arrangement of atoms gives a recognizable shape that is unique to each molecule, and X-ray diffraction helps to elucidate the preferred molecular structure and the packing arrangement. Ultraviolet, infrared, and Raman spectroscopies are helpful for diagnosing the presence of functional groups' interactions and the presence of hydrogen bonds that provide a unique spectral fingerprint that enables us to identify and detect various compounds [13,14].

The objective of this work was to evaluate: (1) the effect of the addition of the EOs cinnamon (CN), anise (AS), and orange (OR) in EFs prepared from a chitosan–zein blend (50%:50%); and (2) the relationship of the films' structural matrix with their physical and mechanical properties. The effect of CN, AS, and OR incorporated into EFs was qualitatively tested on fungal growth inhibition.

2. Results and Discussion

2.1. Color, Transparency, and Optical Properties

The effect of the added essential oils on the transparency, chromaticity, and refractive index of the edible films prepared from a chitosan–zein 50:50% blend are presented in Table 1. Adding the EOs into the chitosan films significantly affected ($p < 0.05$) the a^* (redness/greenness) and b^* (yellowness/blueness) values of the films' surface. When EFs were incorporated with OR and CN, the a^* values showed 27% and 6% more negative values, indicating a redness tendency, whereas the EF with AN added showed the highest a^* value among the treatments (greenness tendency). All EFs incorporating EOs increased their b^* values, indicating a yellowness tendency. Polysaccharide films are usually colorless, essential oils show a slightly yellow appearance, and the incorporation of EOs into polysaccharide-based EFs have been reported to affect color and transparency [4,6].

AS showed the highest transparency value and the lowest refractive index of all of the EOs incorporated into an EF. Nevertheless, all edible films presented a refractive index between 1.35 and 1.55, and because they fall in the range 1.35–1.70 they are classified as transparent [15]. The refractive index of EFs incorporating CN or OR showed similar values compared to the EFs without an EO. However, the refractive index of the EF incorporating AS was significantly different ($p < 0.05$) from the values of the EF without an EO, and the EF with CN. Nevertheless, even small changes in the refractive index indicate that EO addition led to structural changes [16]. The visual properties of a film are an important factor for consumer acceptability.

Table 1. Color and transparency of edible films zein–chitosan 50:50% with essential oils.

Edible Film	% T	a*	b*	η
Without oil	88.4 ± 0.7 ^a	−1.34 ± 0.02 ^a	12.4 ± 2.2 ^a	1.45 ± 0.02 ^a
Anise	72.6 ± 1.4 ^b	−1.10 ± 0.01 ^b	22.6 ± 1.3 ^b	1.35 ± 0.02 ^b
Orange	71.6 ± 1.1 ^{b,c}	−1.70 ± 0.02 ^c	27.8 ± 1.2 ^c	1.55 ± 0.01 ^{a,c}
Cinnamon	69.3 ± 1.1 ^c	−1.42 ± 0.01 ^d	28.8 ± 1.3 ^c	1.50 ± 0.02 ^c

Data are the mean ± standard deviation. Superscript letters a–d are used next to reported values, indicating that if the same letter appears in the same column, the values compared are not significantly different ($p > 0.05$). % T: % transparency; a* and b*: chromaticity; η : refractive index.

2.2. Physical Properties

EF thickness (e) and filmogenic suspension density (ρ) changed with EO addition, achieving higher thickness values as compared to the control sample (Table 2). This effect can be partly related to the filmogenic suspension density, because a higher density was determined within these samples. In this regard, Bonilla et al. [17] working with basil reported that the higher density of a filmogenic suspension containing an EO was due to larger molecular contact between the chitosan's CH groups and the oil compounds, weakening the polymer chain aggregation forces, and producing a more open matrix leading to a higher film thickness.

Table 2. Physical properties of edible film (EF) with different types of essential oils.

Edible Film	e (μm)	ρ (g cm^{-3})	WVP ($\text{g mm h}^{-1} \text{m}^{-2} \text{kPa}^{-1}$)	Rq (nm)	Ra (nm)
Without oil	20.02 ± 1.45 ^a	1.33 ± 0.02 ^a	2.92 ± 0.16 ^a	13.94 ± 0.09 ^a	12.63 ± 0.06 ^a
Anise	23.92 ± 0.92 ^b	1.72 ± 0.01 ^b	1.21 ± 0.10 ^b	11.63 ± 0.14 ^b	9.12 ± 0.12 ^b
Orange	21.43 ± 0.51 ^c	1.42 ± 0.02 ^a	1.62 ± 0.02 ^c	7.24 ± 0.11 ^c	5.64 ± 0.16 ^c
Cinnamon	22.54 ± 0.32 ^d	1.54 ± 0.02 ^c	1.53 ± 0.20 ^{b,c}	3.62 ± 0.12 ^d	2.84 ± 0.09 ^d

Data are the mean ± standard deviation. Superscript letters a–d are used next to reported values, indicating that if the same letter appears in the same column, the values compared are not significantly different ($p > 0.05$). e: EF thickness; ρ : density of solution; WVP: EF water vapor permeability; Ra and Rq: EF roughness.

The film prepared without an EO tended to show higher surface roughness than the others; this could be due to the formation of Z agglomerates, resulting from hydrogen or disulfide bonding and hydrophobic interactions promoted by the pH at which the films' suspensions were prepared. This effect was noted by Escamilla et al. [18] when working with EFs without EO addition, and was confirmed by Guo et al. [19].

The addition of EOs could reduce such interactions, decreasing agglomerates' formation and promoting a smoother surface. The roughness (Ra, Rq) of the EF decreased with the addition of an EO, in agreement with Atarés et al. [20]. These authors worked with films made from soy protein isolate with added ginger and cinnamon EOs and reported that heating enables the integration of the EOs into the protein matrix, resulting in smoother surfaces.

The addition of EOs improved the water vapor barrier property of the chitosan-zein (CT-Z) EF, achieving permeability of 1.2, 1.5, and 1.6 $\text{g mm h}^{-1} \text{m}^{-2} \text{kPa}^{-1}$ for AS, OR, and CN, respectively (Table 2). Aguirre et al. [21], working with whey protein isolate and the oregano EO, suggested a protein–EO interaction that immobilized the protein chain, producing a more ordered and tightly crosslinked structure, and consequently a lower permeability. On the other hand, the interaction of EO components such as ethers, ketones, and aldehydes with the OH groups of polymers increased the EFs' hydrophobicity, thereby improving the water vapor barrier property [22].

Another study produced sodium caseinate films incorporating the cinnamon or ginger EOs, and the cinnamon EO was homogeneously distributed in the protein matrix, whereas the ginger oil droplets showed agglomeration [20]. These authors concluded that structural differences linked to the oil type were the result of complex interactions taking place among lipids, proteins, and solvents. Another study reported that water vapor permeability (WVP) depends on different structural factors,

such as the kind of matrix, the composition and amount of oil added, interactions with the polymers, and the hydrophilic–hydrophobic balance in the matrix [23].

Nevertheless, one report concluded that a decrease in the WVP of chitosan (CT)-based films with a lemongrass, thyme, or cinnamon EO added was due to an increase in the tortuosity factor of the water transfer within the film matrix [24]. Bonilla et al. [17] reported a decrease in the WVP of CT films with an increasing concentration of the basil EO, suggesting that the water molecules' diffusivity decreased because of the hydrophobic nature of the EOs that predominated over the cohesion forces of the CT matrix.

Mechanical Properties

The addition of EOs decreased the elastic modulus and increased the hardness of the EF without an EO. All EFs incorporating an EO did not show a significant difference in the elastic modulus, whereas the AS EF exhibited the highest hardness value (Table 3). The addition of lemongrass, rosemary pepper, and basil EOs decreased the elastic modulus of a cellulose-based EF, suggesting that the interactions of EF polymers with an EO were similar to those exerted by plasticizers [25]. An EF made from fish skin gelatin with added CN, basil, plai, and lemon EOs showed a decreased elastic modulus, but a larger elongation at break due to the replacement of protein–protein interactions by EO addition in the film network [26]. This report agrees with that of Zinoviadou [26], who worked with whey protein with the oregano EO added. In this regard, the three-dimensional structure of proteins stabilized by hydrogen and disulfide bonds should be disrupted to obtain separate, entangled macromolecules to achieve plastic-like properties. The EO and other plasticizers are able to reduce the inter- and intra-molecular interactions and increase films' flexibility depending on the oil and protein compatibility [20].

Table 3. Mechanical properties of zein–chitosan films with essential oils added.

Edible Film	Hardness (MPa)	Elastic Modulus (MPa)
Without oil	5.91 ± 0.41 ^a	66 ± 6 ^a
Anise	104.33 ± 3.22 ^b	22 ± 3 ^b
Orange	57.51 ± 2.43 ^c	20 ± 2 ^b
Cinnamon	25.54 ± 1.85 ^d	24 ± 3 ^b

Data are the mean ± standard deviation. Superscript letters a–d are used next to reported values, indicating that if the same letter appears in the same column, the values compared are not significantly different ($p > 0.05$).

2.3. X-ray Diffraction

To confirm structural changes in an EF matrix, X-ray diffraction and Raman spectroscopy analyses were conducted. EFs prepared without EO addition showed two well-defined peaks, one at 7.5° and the other at 20° (2θ); however, regarding EO-containing films, two peaks, one at 2.7° and another at about 10° (2θ), can be noted.

Based on Equation (14), AS addition promoted higher crystallinity than the other EOs added to the EFs, which was probably associated with higher components miscibility in the films' matrix [27]. On the other hand, OR added to an EF barely decreased the crystallinity (% C: 21.0 ± 0.4 vs. 22.4 ± 0.5) (Figure 1). According to Sánchez-Gonzalez et al. [28], an EO added to an EF based on CT only increased the crystallinity up to 50%, whereas glycerol increases resulted in a lower EF crystallinity due to the higher mobility of the polymer chains [27].

Thus, it is suggested that the presence of OR leads to a decreased crystallinity of the prepared films. This phenomenon corresponds to newly formed interactions between CT and OR that slightly destroy the original crystalline structure, whereas AS and CN incorporation increased the crystallinity, suggesting that AS and CN reinforced CT films, leading to more dense crystalline domains in comparison to pure CT and CT–OR; similar results have been reported by Jahed et al. [29].

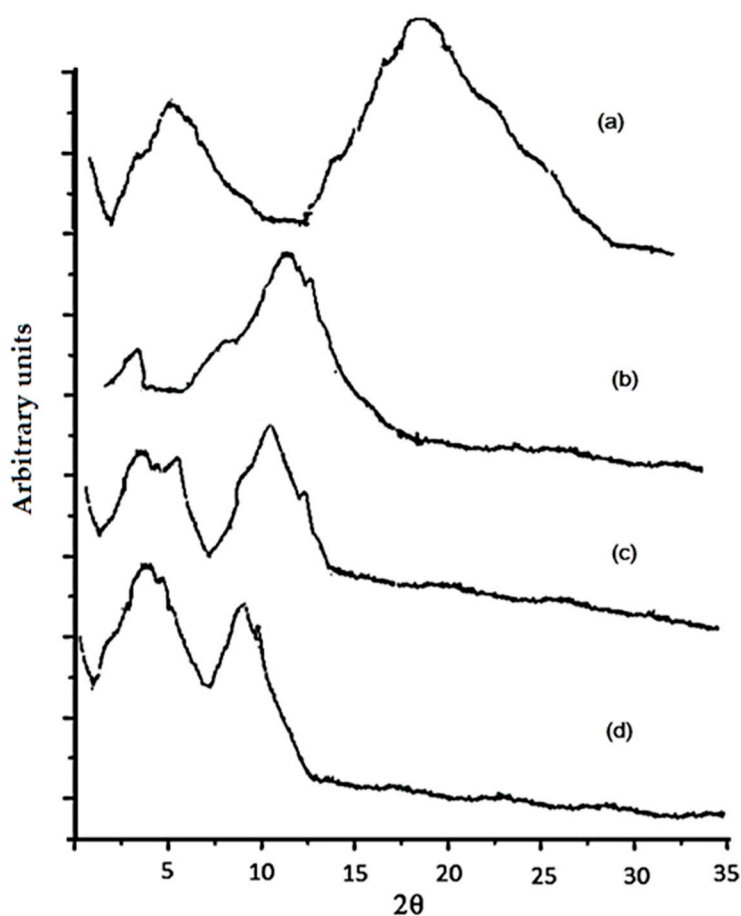


Figure 1. X-ray diffractograms of EF based on a mixture of zein–chitosan (a) Without essential oil (% C = 22.4 ± 0.5); (b) With the cinnamon (CN) essential oil (% C = 27 ± 0.3); (c) With the anise (AS) essential oil (% C = 32 ± 0.2); (d) With the orange (OR) essential oil (% C = 21.0 ± 0.4).

2.4. Raman Spectroscopy

Raman spectroscopy showed that, for all EFs with an EO added, the signal at 1745 cm^{-1} disappeared (Figure 2a), which, according to Gizem-Gezer et al. [30], is a characteristic Z signal that corresponds to the functional group O=S=O. This was attributed to interactions between the protein and EO components.

The signal at 1666 cm^{-1} was associated with the partial acetylation of the NH_2 group of CT [31]; it also disappeared in the presence of an EO.

In relation to CN edible films, cinnamaldehyde, which is comprised of a mono-substituted benzene ring, an aldehyde functional group, and a conjugated double bond, reacted with CT, promoting a nucleophilic addition reaction typical of aldehydes (Figure 2b). When analyzing the EF's structural components, the carbonyl group (C=O) provides a reactive site for nucleophilic addition, with a Schiff base (N=C) formation.

The presence of carbonyl and amino primary groups with a free electron pair allows for the formation of a Schiff base due to the electron-deficient carbonyl carbon. This was confirmed by the disappearance of the characteristic carbonyl (C=O) signal at 1745.9 cm^{-1} when the CN EO was added, which involved a signal decrease at $998\text{--}953\text{ cm}^{-1}$ and at $1081\text{--}1083.7\text{ cm}^{-1}$, both characteristic of C–O–C bonds. This finding agrees with those reported by Gao et al. [32], who studied reactions between aldehydes and CT, nucleophilic addition being the most typical reaction.

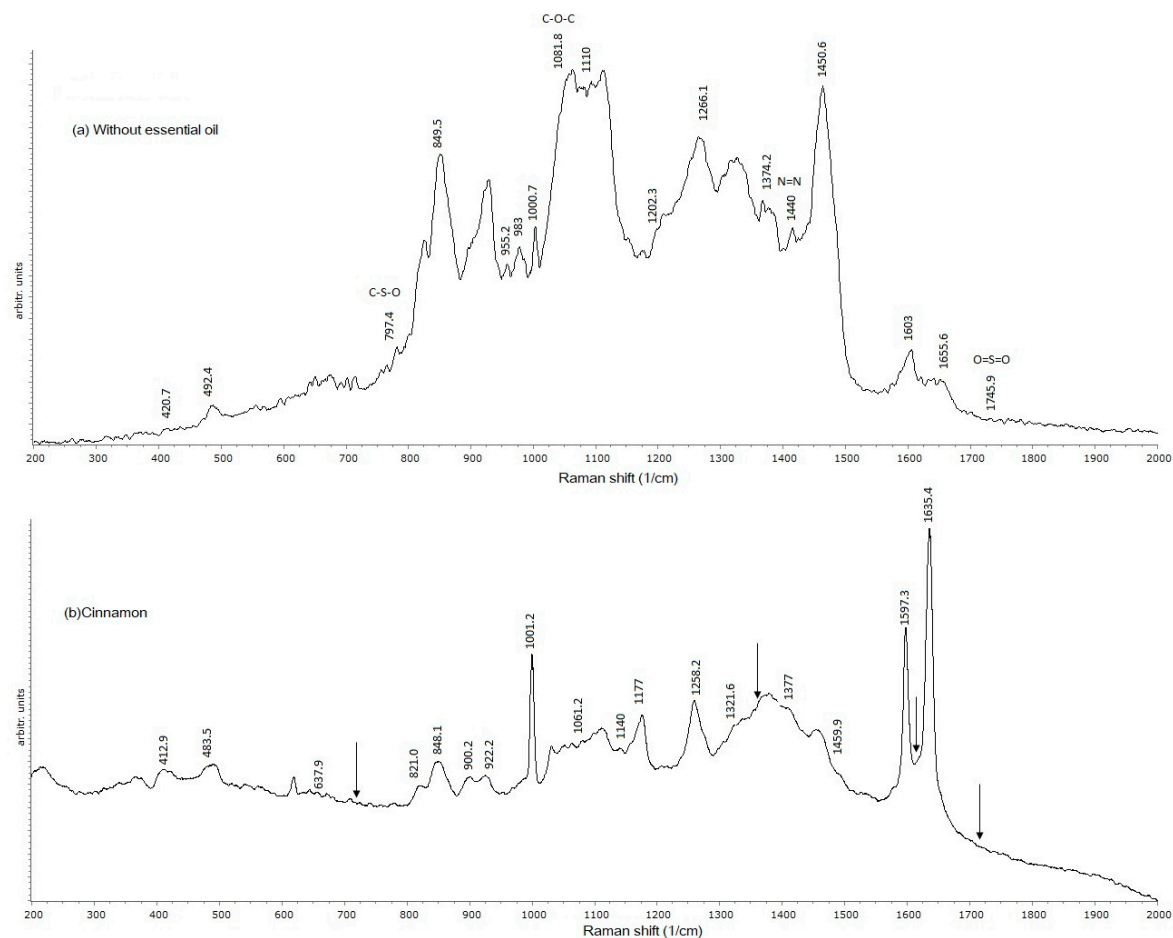


Figure 2. Spectrograms of EFs based on a mixture of zein–chitosan (1:1 *w/w*). (a) Without essential oil; (b) With cinnamon essential oil. Arrows indicate the disappearance of zein signals.

The spectrogram of the edible film containing the OR EO (Figure 3a) did not show characteristic signals at 1081, 1440, and 1745.9 cm^{-1} associated with the C–O–C, N=N, and O=S=O bonds, respectively. Limonene (an olefin) is the main active component of the OR EO, which in the presence of CT experiences olefin metathesis allowing for the synthesis of small and polymeric molecules by scission and the regeneration of C=C molecules [33], which were detected at 1597 cm^{-1} , whereas the signals listed above disappeared.

The EF with the AS EO added showed signal disappearance at 729.74 (C–S), 1110–1150 (C–O–C), 1440 (N=N), and 1745 (C=O). These signal losses indicate the interaction of EF components (CT–Z) with the AS EO, causing bond disruption. The characteristic tyrosine signal disappeared upon the addition of the AS EO (821 cm^{-1}), as well as the signal at 1745.9 cm^{-1} that is related to the Z functional group O=S=O reacting with CT [30] (Figure 3b). This implies the disruption of the protein’s secondary structure (α -helix) [34] so that protein structural changes due to EO addition allow for a tyrosine reaction with other film components. The reduced signal at 1619.4–1655.4 cm^{-1} indicates chemical interactions due to C=N bonds losses. The addition of each EO resulted in a signal disappearance at 729.74 cm^{-1} , characteristic of the C–S aliphatic group of cysteine, suggesting the reaction of each one of the three EOs with the CT–Z EF.

From the Raman spectra, the addition of any EO confirms the X-ray analysis, since an EF’s structure was modified through the formation of a Schiff base, metathesis of CT, or disappearance of CS bonds.

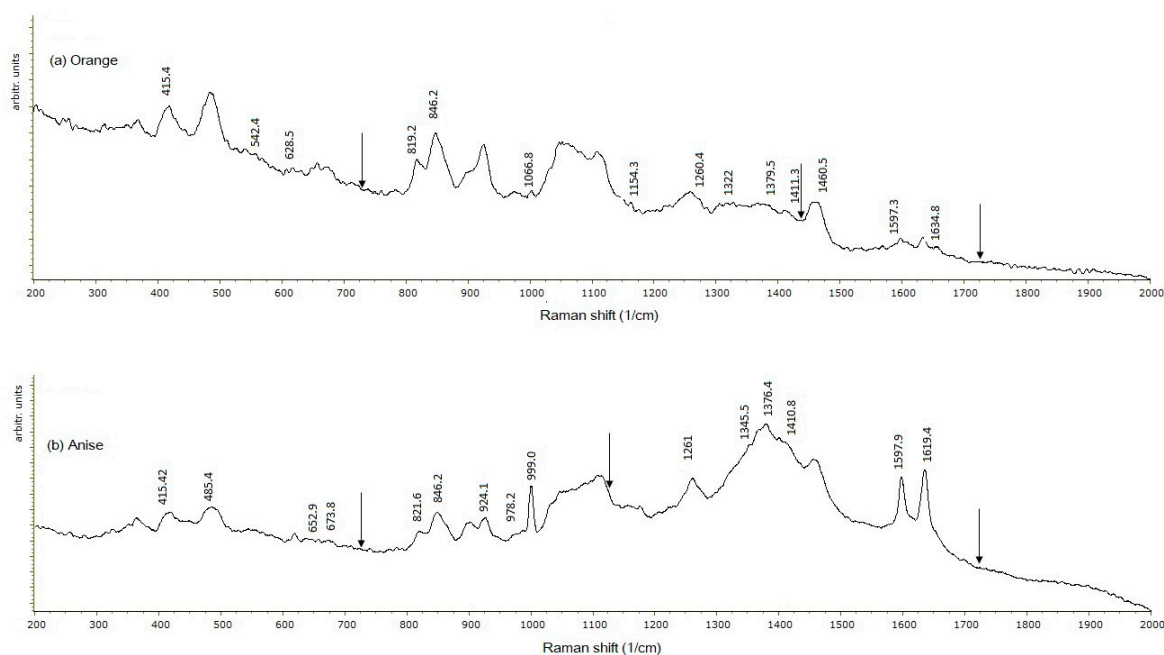


Figure 3. Spectrograms of EF based on a mixture of zein–chitosan (50%:50% *w/w*). (a) With orange essential oil; (b) With anise essential oil. Arrows indicate the disappearance of zein signals.

2.5. Antifungal Activity

All EFs with an EO added showed inhibitory effects against *Rhizopus* sp. and *Penicillium* sp., whereas AS and CN showed an inhibitory effect on *Penicillium* sp., though a lower antifungal effect was observed for *Rhizopus* sp. (Table 4). The inhibitory effect of the AS EO was attributed to anethole, its main bioactive compound [8], which is effective against mycotoxigenic fungi, such as *Rhizopus* sp. and *Penicillium* sp. [7]. Among the EOs, OR showed the smallest inhibitory effect on each of the two tested fungi. The amount of each EO used to conduct the antifungal tests was 15.6 ppm, which is below the daily ingestion limit of 250 ppm [35]. Thus, higher doses may be more effective against these fungi without exceeding the permitted level. Concentrations of 100 ppm of anethole inhibited *Aspergillus flavus* and *Aspergillus parasiticus*, whereas a complete inhibition was achieved using concentrations of 100 ppm and 200 ppm, respectively [36].

Table 4. Inhibitory effect of EFs with different added essential oils.

Edible Film	Average Diameter (cm)	
	<i>Penicillium</i> sp.	<i>Rhizopus</i> sp.
Without essential oil	0	0
Anise essential oil	2.2 ± 0.2 ^a	1.5 ± 0.3 ^a
Cinnamon essential oil	1.9 ± 0.3 ^a	1.7 ± 0.3 ^a
Orange essential oil	0.7 ± 0.1 ^b	0.6 ± 0.2 ^b

Data are the mean ± standard deviation. Superscript letters a-b are used next to reported values, indicating that if the same letter appears in the same column, the values compared are not significantly different ($p > 0.05$).

Anethole targets a fungi's mitochondrial defense system against oxidative stress [37]. The antifungal activity of the EO has been observed at different stages of a fungi's life cycle, including at spore germination, the formation of penetrating structures, and mycelium and sporulation development [38]. Limonene is the active ingredient of OR, and it causes changes in a microbial cell membrane's properties, increasing its fluidity, and leading to altered permeability and homeostasis loss. In addition, the EO

components of OR denature enzymes responsible for germination and sporulation. A concentration of 500 ppm of OR produced a fungistatic effect on *A. flavus* [28].

Cinnamaldehyde is the active compound of CN, and its mechanism of action involves cellular ultrastructural changes, including organelles disappearance and solidification and the degeneration of the cell wall and cytoplasm. An inhibitory concentration of 0.5% (*v/v*) was found against *A. niger* [38].

Although EOs' mechanism of action is not well-defined yet, their inhibitory effect has been generally associated with their hydrophobicity, which causes changes in the permeability, ion transport, and solubilization of lipid components of the cell membrane. More studies are needed to evaluate the combined effect of the tested EOs to ascertain whether there are synergistic effects against a variety of fungi.

Microbial food spoilage is one of the main problems of the food industry, and more than 50% of fruits and fruit products, are spoiled by fungi; in the baking industry, these losses represent between 1% and 3%. In addition, antifungal packaging has been proposed to extend the safety and shelf life of ready-to-eat foods [39]. Thus, active edible films may represent a good alternative for food preservation in the baking and fruit industry, and are suitable for direct food products consumption.

3. Materials and Methods

3.1. Materials

Anise (Essencefleur, Aceites y Esencias Cat. No. 98019, Ciudad de Mexico, Mexico), cinnamon (Essencefleur, Cat. No. 91041) and orange (Essencefleur, Cat. No. 10002) EOs were used. Chitosan ($\geq 75\%$ deacetylation, molecular weight of 375 kDa, Sigma-Aldrich, St. Louis, MO, USA), Zein (Ingredion, San Juan del Río, Qro., Mexico), *Penicillium* sp., and *Rhizopus* sp. were acquired from the type culture collection of the Escuela Nacional de Ciencias Biológicas (ENCB, IPN, Ciudad de Mexico, Mexico).

3.2. Films Preparation

Suspensions of CT (1% CT in 1 N acetic acid, *w/v*), and Z (1:10, Z:ethanol, *w/v*), were prepared by mixing in a hot plate (Barnstead, Thermolyne, MN, USA) for 15 min at 200 rpm at 90 °C; these solutions were mixed in a 1:1 ratio. Three different EFs were elaborated incorporating an EO (AS, CN, and OR) to promote ingredients solubilization and films formation; the pH was adjusted to 9.4 with 0.5 M NaOH [40]. An AS, an OR, or a CN EO was added to reach 250 ppm and was mixed for 10 min at room temperature (~24 °C). Glycerol (Sigma-Aldrich) was added at a 3:1 ratio (Z:glycerol, *w/w*) and stirred for 10 min for complete homogenization. Finally, 10 g of the CT-Z-EO mixtures were poured into petri dishes (90 × 15 mm) and dried in a convection oven (Terlab, Puebla, Mexico) at constant relative humidity (RH) (45%) and temperature (40 °C) for 24 h, according to Abugoch [41]. All samples were separated from the dishes and stored at constant RH (59.7%) and temperature (20 °C) until further analysis.

3.3. Physical Characterization

3.3.1. Color, Transparency, and Optical Properties

The films' thickness, absorption coefficient, and refractive index were determined according to Murray and Dutcher [42] with modifications. Briefly, an ellipsometer (Uvisell LT M200 AGMS, Yvon Horiba, Longjumeau, France) at a 250 to 800 nm wavelength was used. The refractive index and thickness were evaluated by the polarization changes of incident light beams (70 °C) on the surface of the film; these changes consider the ellipsometric angles of the equipment (Δ and Ψ), which in turn are related by mathematical models (polymer and amino acids) included in the software of the same company providing the values of the refractive index and thickness for the equipment. A second method was used to confirm the ellipsometer results by using a precision digital micrometer (IP54, Newton, MA, USA), that was employed to measure five different zones of the films at random

locations. EF transparency and color were determined by using a colorimeter (CR-400 Chroma Meter, Konica Minolta, Tokyo, Japan) with a D65 illumination source at a 0° viewing angle, white background, and by assuming that a completely transparent film will generate the same luminosity values (L^*) as those obtained from the white calibration plate ($L^* = 100$) and that any difference will be the result of a more opaque material ($L^* < 100$); then, lightness is considered as equal to transparency. In this experiment, the film was placed over the calibration plate and measurements were performed at five different points of the film (center and outer parts) avoiding the edges [18]. Prior to the formation of the films, samples of each of the solutions were taken (CT-Z with and without an EO) and their density was evaluated as described by ASTM D1217-12 [43]. In a pycnometer (10 mL) at constant weight, 10 mL of the filmogenic solution was poured, the weight was determined, and the density was obtained by Equation (1):

$$\rho = \frac{m}{v} \quad (1)$$

where ρ is the solution density, v is the volume (10 mL), and m is the mass of 10 mL of solution.

3.3.2. Atomic Force Microscopy (AFM)

AFM provides relative and absolute roughness measurements and allows investigators to obtain three-dimensional (3D) images showing the topographic characteristics of the sample. For this evaluation, an atomic force microscope (Multimode V, Veeco, CA, USA) was used, and the tapping method was applied using silicon probes (RTESP Bruker cantilevers, Santa Barbara, CA, USA) with a resonance frequency of 286–362 kHz and a spring constant of 20–80 N m⁻¹. Samples of 0.5 × 0.5 cm were used and three areas of 5 × 5 μm were scanned at a speed of 1 Hz and resolution of 256 × 256 pixels. Roughness was calculated (Equations (2) and (3)), using the Nano Scope Analysis 1.20 program (Veeco) and applying a flattening process (one grade).

$$Rq = \sqrt{\frac{\sum (Z_i^2)}{N}} \quad (2)$$

$$Ra = \frac{1}{N} \sum_{j=1}^N Z_j \quad (3)$$

where Z_i is the height deviation from the mean of heights, Z_j is the maximum vertical distance between the highest and lowest data points in the image prior to the planefit, Rq is the standard deviation of the Z_i values, Ra is the arithmetic average of the absolute values of the surface height deviations measured from the mean plane, and N is the number of points in the image [44].

3.3.3. Water Vapor Permeability

Water vapor permeability was evaluated using the gravimetric method ASTM E 96–80 [45] with modifications. Slight amounts of water may accumulate on the surface of hydrophilic edible films using the cup method, and the resistance of the stagnant air layer between the bottom side of the film and the surface of the saturated salt may be significant, and, if neglected, may underestimate the water vapor transmission rate (WVTR) [18,46]. Permeability cups with an open mouth of known area (A) were used. The film was sealed on top of a permeation cup, and placed in a desiccator with a saturated NaCl solution at constant temperature (25 °C) and RH (75%). The cups contained a saturated KNO₃ solution (HR = 95.6%), and were weighed at 1 h intervals until equilibrium was reached. The slope of the weight loss (W_s) versus time (t) plot was obtained by linear regression, and the measured WVTR ($WVTR_m$) was calculated (Equation (4)).

$$WVTR_m = \frac{W_s}{tA} \quad (4)$$

The corrected WVTR (WVTR_C) was obtained following Gennadios et al. [47] using Equations (5)–(9).

$$WVTR_C = WVTR_m \times \frac{P_{w1} - P_{w2}}{P_{w3} - P_{w4}} \quad (5)$$

$$P_{w1} = P_0 \times \frac{RH_1}{100} \quad (6)$$

$$P_{w2} = P_0 \times \frac{RH_2}{100} \quad (7)$$

$$P_{w3} = P_T - (P_T - P_{w1}) \frac{WVTR \times R \times T \times h_i}{P_T \times D} \quad (8)$$

$$P_{w4} = P_T - (P_T - P_{w2}) \frac{WVTR \times R \times T \times h_0}{P_T \times D} \quad (9)$$

where A is the cross-sectional area of the film, P_{w1} is the partial pressure inside the permeability cell, P_{w2} is the partial pressure inside the desiccator, P_{w3} and P_{w4} are the pressures below and above the edible film, respectively, D is the diffusivity of water vapor through the air (2.82 m²/d), R is the gas constant, T is the temperature (298 K), and P_T is the atmospheric pressure (85 kPa in Querétaro, Mexico).

The water vapor permeability (WVP) was calculated according to Gennadios et al. [47] and Alvarado-González et al. [46] (Equation (10)).

$$WVP = WVTR_C \frac{L}{P_{W1} - P_{W2}} \quad (10)$$

where WVP is the water vapor permeability (g mm h⁻¹ m⁻² kPa⁻¹), L is the film thickness (mm), and p_{W1} and p_{W2} are the water vapor partial pressures (kPa) over and under the film's surface, respectively.

3.3.4. Mechanical Properties

The mechanical properties evaluated were elastic modulus and hardness. These properties were obtained by a nanoindenter (CSM, Peseux, Switzerland) measuring eight different parts of the films, including the edges and central parts. The indentation conditions were: a maximum load of 2.5 mN at loading and unloading rates of 7.5 mN/min, and a pause of 35 s using a Berkovich tip of known contact area (A_c). From the load-displacement curve, the maximum load (P_{max}), maximum penetration depth (h_{max}), and stiffness of the material (h_s) were obtained. Using these parameters, values of hardness (Equation (11)) and elastic modulus were evaluated (Equations (12) and (13)) [46].

$$H = \frac{P_{max}}{A \times hc} \quad (11)$$

$$E_r = \frac{S\sqrt{\pi}}{2\sqrt{A_c}} \quad (12)$$

$$E_m = \frac{1 - v^2}{\frac{1}{E_r} - \frac{1 - v_i^2}{E_i}} \quad (13)$$

where H (MPa) is the material hardness, E_m is the elastic modulus (GPa), E_r is the reduced modulus, S is the initial unloading stiffness in the load curve, hc is the difference between h_{max} and h_s , v is the Poisson's ratio for polymeric samples estimated as 0.35, and E_i and v_i are the elastic modulus (1141 GPa) of the indenter and Poisson's ratio (0.07), respectively [47].

3.4. Spectroscopic Evaluation

3.4.1. X-ray Diffraction

To determine the percentage of crystallinity, an X-ray diffractometer (PANalytical XPert PRO, Almelo, Netherlands) with a Cu K α radiation line ($\alpha = 1.5418 \text{ \AA}$) was used. Measurements were performed in Bragg–Bretano (θ to 2θ) symmetric geometry from 3° to 35° at steps of 0.01° , a time step of 100 s, 45 kV, and 40 mA for tube power. In addition, a slot of 0.5° of divergence, a Soller slit of 0.04 rad, and a mask of 10 mm were used. For optical diffraction, a pixel (2.5°) and an ultrafast X-ray detector were used to improve the quality of the diffraction pattern [18]. The percentage crystallinity (% C) (Equation (14)) was evaluated considering the crystalline and amorphous peaks.

$$\% C = \frac{I_c}{I_c + I_a} \times 100 \quad (14)$$

where I_c is the area of the crystalline peak, and I_a is the area of the amorphous peak.

3.4.2. Raman Spectroscopy

To study the chemical interactions of an EF's components, Raman spectroscopy was used. This is a high resolution photonic technique that provides chemical and structural information of organic or inorganic compounds by plotting the intensity of the emitted signal relative to the wave number where it is emitted, resulting in the identification of functional groups from the characteristic spectral patterns of the samples [48]. The films were prepared on top of a glass slide, which contained 5-mm thick glass frames along the slide's perimeter, with the purpose of preventing sample spillage. Five milliliters of the sample solution was poured on the slide, and then the samples were dried and stored as directed in Section 3.2. The analysis was carried out using a Raman spectrophotometer (Raman Olympus BX41, Horiba, Edison, NJ, USA) coupled to an Olympus BX 41 microscope with a $50\times$, N.A. 0.55 objective. Film samples were irradiated with a 735 nm emission laser, with diffraction limited to 702 m. The spectral resolution was 0.16 cm^{-1} at a 633 nm excitation wavelength, with a 1800 g/mm and charged coupled device detector, which showed enhanced quantum efficiency in the 450–950 nm spectral range. The confocal hole and entrance slit of the monochromator were fixed at 400 μm . Readings were carried out in a spectral interval of 400 to 2000 cm^{-1} . The Spekwinn 32 software (developer: F. Menges, Oberstdorf, Germany) was used for data treatment.

3.5. Microbiological Analysis

Microbiological analysis was performed following Boonruang [49], with modifications. Fungi spores were taken from a stock culture and incubated in PDA plates at 30°C for 15 day to enhance sporulation. Two milliliters of sterile 0.05% (w/v) Tween 80 was added to each plate surface, and the spore suspensions were collected, followed by an adjustment to 1×10^7 spores/mL. For the agar disc diffusion method, edible films were cut (0.5 cm diameter) and PDA plates were inoculated by smearing 100 μL of *Penicillium* sp. or *Rhizopus* sp. spores suspension and left to dry for 60 min in a laminar flow cabinet. Three edible film discs for each fungus were sterilized by placing them in the laminar flow cabinet under UV light (260 nm) for 30 min, at a distance of 30 cm, followed by placing them on the inoculated agar surface. From preliminary Raman studies, we did not find any difference between irradiated and non-irradiated films. The plates were incubated 72 h at 30°C , and microbial growth was determined by measuring the inhibition zone diameter.

3.6. Statistical Analysis

All parameters are expressed as the mean value and its corresponding standard deviation. For each analysis, three independent films were tested, and they were evaluated at least at three different points (edges and center). Data were analyzed by one-way analysis of variance (ANOVA)

using the SigmaStat 3.5 software (San Jose, CA, USA). Significant differences were determined using the Tukey test, with significance at $p < 0.05$.

4. Conclusions

EOs added to EFs based on CT-Z produced more elastic, harder, and crystalline films with enhanced mechanical and barrier properties. Improved physical properties were the result of chemical interactions among the reactive groups of film components, such as amino acids from zein (cysteine and tyrosine), glucosamine from CT, and cinnamaldehyde, anethole, or limonene from EOs.

In particular, these EFs showed inhibitory effects against food spoilage fungi, such as *Penicillium* sp. and *Rhizopus* sp. Disrupted tyrosine bonds were found in the EF with AS added, which in addition to the disappearance of cysteine C–S bonds likely contributed to decrease the WVP. Thus, in this study, the properties of the EFs with any of the incorporated EOs tested suggest that such EFs may represent a good alternative for a variety of food applications.

Acknowledgments: Monserrat Escamilla-García wishes to express their gratitude to CONACyT and PIFI-IPN for the scholarship provided. This research was financed through the projects 20131518, 20151340, and 20151383 from the Instituto Politécnico Nacional (IPN-México) and the project 133102 from CONACYT.

Author Contributions: Monserrat Escamilla-García carried out the experimental part of the research project and the manuscript's writing. Georgina Calderón-Domínguez conducted the Raman spectroscopy and X-ray diffraction analyses and their interpretation. José Jorge Chanona-Pérez collaborated on the interpretation of the Raman spectroscopy analysis and ellipsometer measurements. Angélica G. Mendoza-Madriral collaborated on the AFM measurements and their interpretation. Prospero Di Pierro designed experiments and selected physicochemical tests. Blanca E. García-Almendárez and Aldo Amaro-Reyes developed the microbiological experiments and their interpretation. Carlos Regalado-González advised on the planning of the experiments and the manuscript's writing.

Conflicts of Interest: The authors declare no conflict of interest.

References

1. Licciardello, F. Packaging, Blessing in Disguise. Review on Its Diverse Contribution to Food Sustainability. *Trends Food Sci. Technol.* **2017**, *65*, 32–39. [[CrossRef](#)]
2. Ganiari, S.; Choulitoudi, E.; Oreopoulou, V. Edible and Active Films and Coatings as Carriers of Natural Antioxidant for Lipid Food. *Trends Food Sci. Technol.* **2017**, *68*, 70–82. [[CrossRef](#)]
3. Ribeiro-Santos, R.; Andrade, M.; Ramos de Melo, N.; Sanches-Silva, A. Use of Essential Oils in Active Food Packaging: Recent Advances and Future Trends. *Trends Food Sci. Technol.* **2017**, *61*, 132–140. [[CrossRef](#)]
4. Zhang, S.; Zhang, M.; Fang, Z.; Liu, Y. Preparation and Characterization of Blended Cloves/Cinnamon Essential Oil Nanoemulsions. *LWT-Food Sci. Technol.* **2017**, *75*, 316–322. [[CrossRef](#)]
5. Pina-Pérez, M.; Martínez-López, A.; Rodrigo, D. Cinnamon Antimicrobial Effect Against *Salmonella typhimurium* Cells Treated by Pulsed Electric Fields (PEF) in Pasteurized Skim Milk beverage. *Int. Food Res. J.* **2012**, *48*, 777–783. [[CrossRef](#)]
6. Noshirvani, N.; Ghanbarzadeh, B.; Garrat, C.; Rezaei, M.; Hashemi, M. Cinnamon and Ginger Essential Oils to Improve Antifungal, Physical and Mechanical Properties of Chitosan-Carboxymethyl Cellulose Films. *Food Hydrocoll.* **2017**, *70*, 36–45. [[CrossRef](#)]
7. Matan, N.; Matan, N. Antifungal Activities of Anise Oil, Lime Oil and Tangerine Oil against Molds on Rubberwood (*Hevea brasiliensis*). *Int. Biodeterior. Biodegrad.* **2008**, *62*, 75–78. [[CrossRef](#)]
8. Kosalec, I.; Pepeljnjak, S.; Kuš, S. Antifungal activity of fluid extract and essential oil from anise fruits (*Pimpinella anisum* L., *Apiaceae*). *Acta Pharm.* **2005**, *5*, 377–385.
9. Matan, N. Antimicrobial activity of edible film incorporated with essential oils to preserve dried fish (*Decapterus maruadsi*). *Int. Food Res. J.* **2012**, *19*, 1733–1738.
10. Acar, Ü.; Kesbic, O.S.; Yilmaz, S.; Gültepe, N.; Türker, A. Evaluation of the Effects of Essential Oil Extracted from Sweet Orange Peel (*Citrus sinensis*) on Growth Rate of Tilapia (*Oreochromis mossambicus*) and Possible Disease Resistance Against *Streptococcus iniae*. *Aquaculture* **2015**, *437*, 282–286. [[CrossRef](#)]
11. Velázquez-Nuñez, M.; Ávila-Sosa, R.; Palou, E.; López-Malo, A. Antifungal Activity of Orange (*Citrus sinensis* var. *Valencia*) Peel Essential Oil. *Food Control* **2013**, *31*, 1–4. [[CrossRef](#)]

12. Evageliou, V.; Saliari, D. Limonene Encapsulation in Freeze Dried Gellan Systems. *Food Chem.* **2017**, *223*, 72–75. [[CrossRef](#)] [[PubMed](#)]
13. Duncan, T. Applications of Nanotechnology in Food Packaging and Food Safety: Barrier Materials, Antimicrobials and Sensors. *J. Colloid Interface Sci.* **2011**, *363*, 1–24. [[CrossRef](#)] [[PubMed](#)]
14. Chandrasekaran, R. X-ray Diffraction of Food Polysaccharides. *Adv. Food Nutr. Res.* **1998**, *42*, 131–210. [[CrossRef](#)] [[PubMed](#)]
15. Coso, R.; Solís, J. Relation between Nonlinear Refractive Index and Third-Order Susceptibility in Absorbing Media. *J. Opt. Soc. Am. B* **2004**, *21*, 640–644. [[CrossRef](#)]
16. Loftalian, A.; Jandaghian, A.; Saghafifar, H.; Mohajerani, E. Young's Modulus Measurement Based on Surface Plasmon Resonance. *Opt. Laser Technol.* **2017**, *94*, 248–252. [[CrossRef](#)]
17. Bonilla, J.; Vargas, M.; Atarés, L.; Chiralt, A. Physical Properties of Chitosan-Basil Essential Oil Edible Films as Affected by Oil Content and Homogenization Conditions. *Procedia Food Sci.* **2011**, *1*, 50–56. [[CrossRef](#)]
18. Escamilla-García, M.; Calderón-Domínguez, G.; Chanona-Pérez, J.J.; Farrera-Rebollo, R.; Andraca-Adame, L.A.; Arzate-Vázquez, I.; Mendez-Mendez, J.V.; Moreno-Ruíz, L. Physical and Structural Characterisation of Zein and Chitosan Edible Films Using Nanotechnology Tools. *Int. J. Biol. Macromol.* **2013**, *61*, 196–203. [[CrossRef](#)] [[PubMed](#)]
19. Guo, X.; Lu, Y.; Cui, H.; Jia, X.; Bai, M.Y. Factors Affecting the Physical Properties of Edible Composite Film Prepared from Zein and Wheat Gluten. *Molecules* **2012**, *17*, 3794–3804. [[CrossRef](#)] [[PubMed](#)]
20. Atarés, L.; Bonilla, J.; Chiralt, A. Characterization of Sodium Caseinate-Based Edible Films Incorporated with Cinnamon or Ginger Essential Oils. *J. Food Eng.* **2010**, *100*, 678–687. [[CrossRef](#)]
21. Aguirre, A.; Borneo, R.; León, A. Antimicrobial, Mechanical and Barrier Properties of Triticale Protein Films Incorporated with Oregano Essential Oil. *Food Biosci.* **2013**, *1*, 2–9. [[CrossRef](#)]
22. Nisar, T.; Wang, Z.C.; Yang, X.; Tian, Y.; Iqbal, M.; Guo, Y. Characterization of Citrus Pectin Films Integrated with Clove Bud Essential Oil: Physical, Thermal, Barrier, Antioxidant and Antibacterial Properties. *Int. J. Biol. Macromol.* **2017**, in press. [[CrossRef](#)] [[PubMed](#)]
23. Acosta, S.; Chiralt, A.; Santamarina, P.; Rosello, J.; González-Martínez, C.; Cháfer, M. Antifungal Films Based on Starch-Gelatin Blend, Containing Essential Oils. *Food Hydrocoll.* **2016**, *61*, 233–240. [[CrossRef](#)]
24. Peng, Y.; Li, Y. Combined Effects of Two Kinds of Essential Oils on Physical, Mechanical and Structural Properties of Chitosan Films. *Food Hydrocoll.* **2014**, *36*, 287–293. [[CrossRef](#)]
25. Rocha Bastos, M.S.; Laurentino, L.S.; Canuto, K.; Guabiraba Mendes, L.; Mota Matin, C.; Frota Silva, S.; Ferro Furtado, R. Physical and Mechanical Testing of Essential Oil-Embedded Cellulose Ester Films. *Polym. Test.* **2016**, *49*, 156–161. [[CrossRef](#)]
26. Zinoviadou, K.; Koutsoumanis, K.; Biliaderis, C. Biopolymer-Based Films as Carriers of Antimicrobial Agents. *Procedia Food Sci.* **2011**, *1*, 190–196. [[CrossRef](#)]
27. Ghasemlou, M.; Khodaiyan, F.; Oromiehie, A. Rheological and Structural Characterisation of Film-Forming Solutions and Biodegradable Edible Film Made from Kefiran as Affected by Various Plasticizer Types. *Int. J. Biol. Macromol.* **2011**, *49*, 814–821. [[CrossRef](#)] [[PubMed](#)]
28. Sánchez-González, L.; Vargas, M.; González-Martínez, C.; Chiralt, A.; Cháfer, M. Use of Essential Oils in Bioactive Edible Coatings. *Food Eng. Rev.* **2011**, *3*, 1–16. [[CrossRef](#)]
29. Jahed, E.; Khaledebed, M.A.; Almasi, H.; Hasanzadeh, R. Physicochemical Properties of *Carum copticum* Essential Oil Loaded Chitosan Films Coating Organic Nanoreinforcements. *Carbohydr. Polym.* **2017**, *164*, 325–338. [[CrossRef](#)] [[PubMed](#)]
30. Gizem-Gezer, P.; Logan-Liu, G.; Kokini, J.L. Development of a Biodegradable Sensor Platform from Gold Coated Zein Nanofotonic Films to Detect Peanut Allergen, Ara h1, Using Surface enhanced Raman Spectroscopy. *Talanta* **2016**, *150*, 224–232. [[CrossRef](#)] [[PubMed](#)]
31. Zając, A.; Hanuza, J.; Wandas, M.; Dymińska, L. Determination of N-acetylation Degree in Chitosan Using Raman Spectroscopy. *Spectrochim. Acta A Mol. Biomol. Spectrosc.* **2015**, *134*, 114–120. [[CrossRef](#)] [[PubMed](#)]
32. Gao, B.; Wan, M.; Men, J.; Zhang, Y. Aerobic Selective Oxidation of Benzyl Alcohols to Benzaldehyde Catalyzed by Bidentate Shift Base Dioxonolybdenum (VI) Complex Immobilized on CPS Microspheres. *Appl. Catal. A* **2012**, *439–440*, 156–162. [[CrossRef](#)]
33. Meng, X.; Edgar, K. Synthesis of Amide-Functionalized Cellulose Esters by Olefin Cross-Metathesis. *Carbohydr. Polym.* **2015**, *132*, 565–573. [[CrossRef](#)] [[PubMed](#)]

34. Berhe, D.; Engelsen, S.; Hviid, M.; Lametsch, R. Raman Spectroscopy Study of Effect of the Cooking Temperature and Time on Meat Proteins. *Int. Food Res. J.* **2014**, *66*, 123–131. [[CrossRef](#)]
35. Baschieri, A.; Ajvazi, M.D.; Folifack-Tonfack, J.L.; Valgimigli, L.; Amorati, R. Explaining the Antioxidant Activity of Some Common Non-Phenolic Components of Essential Oils. *Food Chem.* **2017**, *232*, 656–663. [[CrossRef](#)] [[PubMed](#)]
36. Ferdes, M.; Al Juhami, F.; Özcan, M.M.; Ghafoor, K. Inhibitory Effect of Some Plant Essential Oils on Growth of *Aspergillus niger*, *Aspergillus oryzae*, *Mucor pusillus* and *Fusarium oxysporum*. *S. Afr. J. Bot.* **2017**, in press. [[CrossRef](#)]
37. Aly, S.; Sabry, B.; Shaheen, M.; Hathout, A. Assessment of Antimycotoxigenic and Antioxidant Activity of Star Anise (*Illicium verum*) in Vitro. *J. Saudi Soc. Agric. Sci.* **2016**, *15*, 20–27. [[CrossRef](#)]
38. Ribes, S.; Fuentes, A.; Talens, P.; Barat, J.M.; Ferrari, G.; Donsì, F. Influence of Emulsifier Type on Antifungal Activity of Cinnamon Leaf, Lemon, and Bergamot Oil Nanoemulsions against *Aspergillus niger*. *Food Control* **2017**, *73*, 784–795. [[CrossRef](#)]
39. Van Long, N.N.; Dantigny, P. *Fungal Contamination in Packaged Foods. Antimicrobial Food Packaging*; Academic Press: Oxford, UK, 2016; pp. 45–59, ISBN 978-12-800723-5.
40. Gao, P.; Wang, F.; Gu, F.; Ning, J.; Liang, J.; Li, N.; Ludescher, R.D. Preparation and Characterization of Zein Thermo-Modified Starch Films. *Carbohydr. Polym.* **2017**, *157*, 1254–1260. [[CrossRef](#)] [[PubMed](#)]
41. Abugoch, L.; Tapia, C.; Villamán, M.; Yazdani-Pedram, M.; Díaz-Dosque, M. Characterization of Quinoa Protein Chitosan Blend Edible Film. *Food Hydrocoll.* **2011**, *25*, 879–886. [[CrossRef](#)]
42. Murray, C.; Dutcher, J. Effect of Changes in Relative Humidity and Temperature on Ultrathin Chitosan Films. *Biomacromolecules* **2006**, *7*, 3460–3465. [[CrossRef](#)] [[PubMed](#)]
43. *Standard Test Method for Density and Relative Density (Specific Gravity) of Liquids by Bingham Pycnometer*; ASTM International: West Conshohocken, PA, USA, 2012; ASTM D1217–12. [[CrossRef](#)]
44. Ghanbarzadeh, B.; Oromiehi, A. Thermal and Mechanical Behavior of Laminated Protein Films. *J. Food Eng.* **2009**, *90*, 517–524. [[CrossRef](#)]
45. American Society for Testing and Materials. Standard Test Method for Water Vapor Transmission of Materials. In *ASTM Book of Standards*; American Society for Testing and Materials: West Conshohocken, PA, USA, 1980; ASTM E96-80. [[CrossRef](#)]
46. Alvarado-González, J.; Chanona-Pérez, J.J.; Welti-Chanes, J.; Calderón-Domínguez, G.; Arzate-Vázquez, I.; Gutierrez López, G.F.; Pacheco-Alcalá, L. Optical, Microstructural, Functional and Nanomechanical Properties of *Aloe vera* Gel/Gellan Gum Edible Films. *Rev. Mex. Ing. Quim.* **2012**, *11*, 193–210.
47. Gennadios, A.; Weller, C.; Gooding, C. Measurement Errors in Water Vapor Permeability of Highly Permeable, Hydrophilic Edible Films. *J. Food Eng.* **1994**, *21*, 395–400. [[CrossRef](#)]
48. Smith, W.E.; Dent, G. *Modern Raman Spectroscopy—A Practical Approach*; John Wiley & Sons: West Sussex, UK, 2005; pp. 11–31.
49. Boonruang, L.; Kerddonfag, N.; Chinsriikul, W.; Mitcham, E.J.; Chohenchob, V. Antifungal Effect of Poly(Lactic Acid) Films Containing thymol and R-(–)-Carvone against Anthracnose Pathogens Isolated from Avocado and Citrus. *Food Control* **2017**, *78*, 85–93. [[CrossRef](#)]



© 2017 by the authors. Licensee MDPI, Basel, Switzerland. This article is an open access article distributed under the terms and conditions of the Creative Commons Attribution (CC BY) license (<http://creativecommons.org/licenses/by/4.0/>).